Advances in air-coupled ultrasonic testing combining an optical microphone with novel transmitter concepts

Jan-Carl Grager[1,2], Daniel Kotschate[3], Jakob Gamper[2], Mate Gaal[3], Katja Pinkert[2], Hubert Mooshofer[1], Matthias Goldammer[1] and Christian U Grosse[2]
[1] Siemens, Corporate Technology, Germany, jan-carl.grager@siemens.com
[2] Technical University of Munich, Chair of Non-destructive Testing, Germany
[3] Bundesanstalt für Materialforschung und -prüfung (BAM), Germany

Abstract

Air-coupled ultrasound (ACU) is increasingly used for automated and contactless inspection of large-scale composite structures as well as for non-destructive testing (NDT) of water-sensitive or porous materials. The major challenge to overcome using ACU in NDT is the enormous loss of ultrasonic energy at each solid-air interface caused by the high acoustic impedance mismatch. Resonant low-frequency piezoceramic transducers are specially designed to achieve high sound pressure levels. For an expanded use of this technique, however, the spatial resolution needs to be increased.

Recent studies of our collaborative research group demonstrated the successful application of a resonance-free, highly sensitive receiver that uses a Fabry-Pérot etalon instead of piezoceramic materials or membranes. However, to reach the full potential of this broadband small-aperture optical microphone, novel transmitter concepts have to be developed and evaluated for advanced NDT applications.

Different types of transmitter were tested in combination with the optical microphone acting as receiver and they were compared to conventional piezoceramic transducers in through-transmission mode. Monolithic carbon fiber-reinforced plastics (CFRP) and CFRP sandwich structures containing different defect types were inspected. Presented results are processed as C-scan images and further evaluated for spatial resolution, signal-to-noise ratio and sensitivity of each measurement setup. Novel transmitter concepts, such as ferroelectret and thermoacoustic emitters, show promising findings with a considerably improved time and spatial resolution for ACU-NDT.

1. Introduction

By now, air-coupled ultrasound has proven to be a very reliable inspection technique for a variety of testing applications where liquid couplants are not preferred or accepted (1). The possibility for contactless and contamination-free inspection makes ACU particularly attractive for many industries and research institutes that aim to test highly attenuative materials or large and complex structures where an automated inspection is the only technically and economically feasible solution (1-3).

In conventional ultrasonic testing, liquid coupling media are used to transfer a sufficient amount of acoustic energy from the transducer to the test object or vice versa. In contrast, ACU utilizes ambient air as couplant. Consequently, the major technical

challenge of air-coupled ultrasound is the high mismatch of the acoustic impedance Z between solids (transducers and test component) and air (couplant) that results in an enormous loss of ultrasonic energy at these interfaces (1, 3). To overcome this difficulty, the technological progress of ACU has always been and will continue to be focused on the development of the transducer technology (1, 3-17).

A previous study in our collaborative research group demonstrated the first application of a new sensing technique for ultrasound (5). A novel optical sensor replaced the resonant piezoelectric receiver probe and its required preamplifier in a commercial ACU system. One air-solid transition in the ACU test configuration could be eliminated and the spatial resolution in the recorded C-scan images increased significantly (5, 6).

This contribution describes the successful application of this novel sensor for air-coupled ultrasonic measurements. The evaluation of its performance in combination with different actuator concepts is of particular concern. For that, monolithic CFRP composites and foam sandwich structures with CFRP facesheets are inspected. In the following, only the robust and well-established through-transmission configuration is considered, although other transducer arrangements are possible as well (1, 3, 5). Three transmitter types are used in this study: first, non-focused and resonant piezoceramic transducers (2, 3); second, charged cellular polypropylene (cPP) probes (also called ferroelectret transducers) (7, 8); and third, a spherically shaped thermoacoustic emitter (9). This variety allows a very comprehensive evaluation of the receiving system itself and its potential in combination with the different transmitter types used in this study.

2. Air-coupled ultrasonic transducers

Several ACU transducer types are available or in development and differ in respect to their physical principle or their construction. The fundamental operating principles of the actuators used in this contribution and of the optical microphone will be explained in this section. Readers that are particularly interested in (other) available probe concepts are referred, e.g. to the works of Chimenti (1) or Nakamura (10).

Bulk piezoceramics or piezo-composites are still widespread ACU transducer materials. To diminish the contrast in acoustic impedance, matching layers of defined Z and thickness ($\lambda/4$) can be applied to the piezoceramic. This, however, creates an inherent narrowband frequency filter in the probe (11). For optimization of the sound pressure level of these transducers, the piezoceramic is often excited with long duration tone-burst signals and may not be damped by a backing material. Consequently, this resonant probe concept tends to produce very long ultrasonic pulses and results in a poor axial (time) resolution (3). Many active (e.g. multi-channel annular arrays (12)) or passive (e.g. shaped transducers or lenses) focusing techniques exist to improve the spatial resolution (13).

For ferroelectret transducers, the mismatch to air is not that prominent as they are based on low-density (~330 kg/m³) and low-velocity (c_L~80 m/s) cellular polypropylene (cPP) foils and hence matching layers can be omitted (see Figure 1a). At common excitation voltages of up to about 2 kV, sound waves are generated by the piezoelectric and by the here more dominant electrostrictive effect (7). The latter mechanism cannot be utilized

for reception. Focusing capabilities are tailored by the aperture size or, e.g. by bonding the cPP foil onto spherically shaped back plates (8). Practical pulse durations of ferroelectret probes are shorter than of resonant piezoceramic transducers (that show long post-pulse oscillations) but are inferior to those of thermoacoustic actuators which have no oscillating mass at all (3, 9).

Novel thermoacoustic (TA) transmitters consist of a solid substrate, such as glass, which is coated with electrically conductive films, like indium-tin-oxide (ITO) (see Figure 1b). An electrical excitation pulse applied to the film heats up the transmitter surface shortly and sound waves emerge due to the transfer of thermal energy to adjacent gas particles. This working principle does not require matching layers and allows the generation of short broadband ultrasonic pulses (14). The solid substrate can also be spherically shaped for focusing purposes (9). In contrast to piezoelectric probes, the thermoacoustic working principle does not enable the detection of ultrasonic waves. Nevertheless, combined thermoacoustic-piezoelectric transducer concepts exist that facilitate, e.g. ACU measurements in a standard pulse-echo configuration (9, 14).

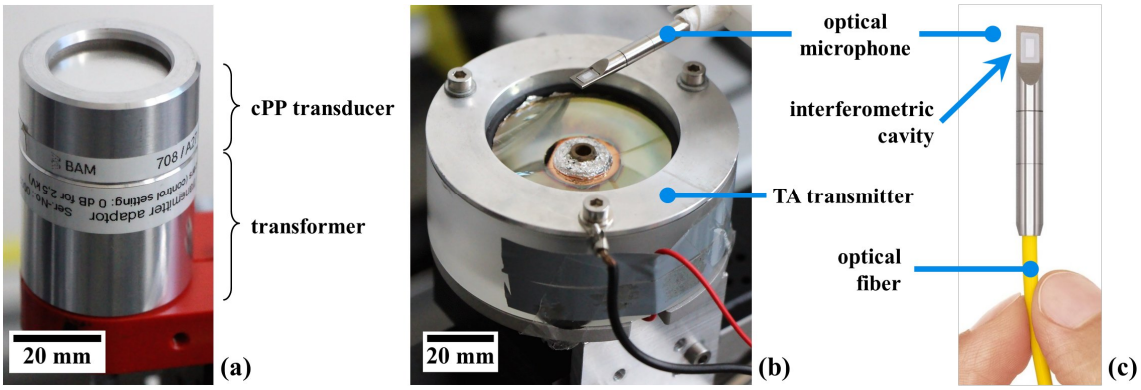

Figure 1. Selection of novel transducer types used in this study showing: (a) a ferroelectret probe based on cellular polypropylene (cPP) foil; (b) a ring-shaped and spherically focused thermoacoustic (TA) transmitter based on indium-tin-oxide with the optical microphone put in place for a characterization of the emitted sound field; (c) a sensor head of the optical microphone with its very small interferometric cavity at the tip of the sensor which is open to the air ((c) reprinted with permission from *XARION Laser Acoustics*).

If an ultrasonic wave propagates through a gas or a liquid not only is the acoustic pressure distribution altered in the medium but also its refractive index and the speed of light. This change can be detected by optical means with novel sensors developed by *XARION Laser Acoustics* (see Figure 1c). Their transducer principle is based on a compact and rigid Fabry-Pérot etalon which is open to the air. At the tip of the sensor head, two parallel semi-transparent mirrors are located in the interferometric cavity. The optical wavelength and the transmission of a laser beam that is sent via an optical fiber to the etalon are altered according to the sound pressure change in the cavity leading to a representative electric signal (15).

The sensors' flat frequency response in the air ranges from about 5 Hz up to 1 MHz (15). This broad frequency range makes it a very promising sensing technique for air-coupled ultrasound, especially for novel broadband actuators such as thermoacoustic transmitters. A significant increase of the spatial resolution of ACU scans is resulting from the tiny aperture size of 2 mm by 0.3 mm. As a side benefit, one air-solid transition is eliminated in the ACU test configuration (6, 15).

3. Experimental configuration

A commercial ACU test instrument from *Ingenieurbüro Dr. Hillger* (USPC AirTech 4000) with a two-axis manipulator system has been used in this study. All C-scans were recorded in through-transmission configuration and processed with Matlab.

The resonant piezoceramic-based transducers (AirTech series) can directly be operated with the ACU test instrument. Operating ferroelectric and thermoacoustic probes with the USPC AirTech 4000 requires some technical adaptations. TA transducers generate the acoustic transmission by heating up the surrounding gas volume, whereas the cPP emitters follow the excitation signal within their mechanical limits and expand and compress the volume of the foil used. In consequence, thermoacoustic emitters require a power source supplying enough electrical power for heating processes. The pulsed power source must be capable of generating fast transient pulses (high slew rate, short rise times) and a high pulse repetition frequency (PRF). The presented measurements were made using a primary power source of 10 kW and an amplifier stage developed at the *Bundesanstalt für Materialforschung und -prüfung*. This amplifier stage can generate excitation pulses lasting up to 10 µs and peak power levels of 15 kW. For ferroelectret transducers, a high-voltage pulse-shaped excitation of 1.8 kV is applied, causing a sound pressure of about 140 dB. Due to the dielectric strength (20 kV/mm), higher electric potentials would damage the foil by inducing electrical breakdowns. Since driving the cPP foil does not require such a high amount of energy, the voltage is generated using a transformer.

Whenever the optical microphone (Eta250 Ultra from *XARION Laser Acoustics*) was used as the receiver, its signal conditioning unit was directly connected to the main amplifier of the USPC AirTech 4000. Also, the separate ultra-low noise preamplifier which is usually positioned close to the resonant receiver probe (3) was then excluded from the test configuration. The spatial resolution was optimized by placing the optical microphone close to the rear surface of the test object (10).

4. Inspection results

The evaluation of the imaging performance of the optical microphone starts with an inspection of a CFRP sample with a quasi-isotropic layup. This test piece consists of 128 plies and measures 22 mm in thickness. Flat-bottom holes (FBHs) from 0.5 mm up to 4.0 mm in diameter are located at different depths (see Figure 2a).

For the through-transmission setup, a pair of planar resonant AirTech transducers with a nominal frequency of 200 kHz was used. Both have an aperture size of 11.1 mm in diameter and a bandwidth of about 10 %. This result is depicted in Figure 2b and compared with C-scans recorded with the optical microphone (see Figures 2c and 2d). Both receivers can clearly resolve the FBHs with a diameter of 4 mm but are not capable of imaging the tiny 0.5 mm and 1 mm reflectors. In Figure 2, it is indicated whether an eighth-order infinite impulse response (IIR) bandpass filter (190 kHz - 210 kHz) was applied to the A-scan data or not. This adjustment of the optical microphones' broad frequency range to the narrow spectrum of the resonant transmitter reduced the dominant noise level in the C-scans (cf. Figures 2c and 2d). Although noise is still prominent in images using the Eta250 Ultra, especially the 2 mm flat-bottom holes can be resolved much better than using the resonant transducer pair.

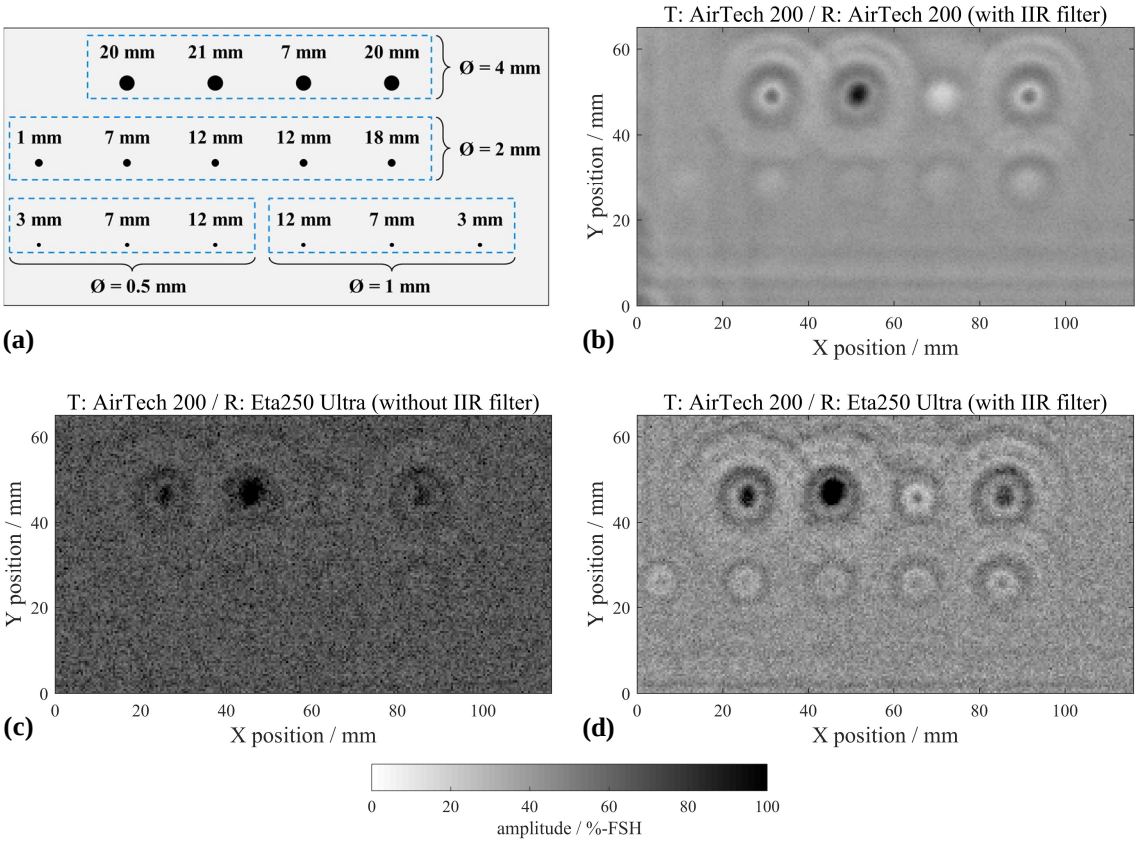

Figure 2. Evaluation of the imaging performance of the optical microphone testing a CFRP sample with flat-bottom holes using a resonant 200 kHz transmitter. The depths of the flat-bottom holes are indicated in (a).

Test frequencies of about 100 kHz and below can be very advantageous to obtain a sufficient penetration power and sensitivity when inspecting highly attenuative sandwich composites with ACU. This, however, can negatively affect the imaging capabilities.

Two sandwich composites with polyurethane foam and 1 mm thick CFRP facesheets (see Figure 3) were tested with resonant AirTech probes having a nominal frequency of 75 kHz, a bandwidth of about 12 % and an aperture size of 30 mm. An eighth-order IIR bandpass filter (70 kHz - 80 kHz) was applied to the A-scan data of all scans, mainly to reduce noise in the processed C-scans in Figures 4b and 5b.

The first test piece has a thickness of 16 mm and is undamaged. An M6 stainless steel plain washer with an inner diameter of 6.4 mm and an outer diameter of 18.0 mm was attached with a rectangular strip of double-sided adhesive tape on the surface of the sandwich sample (see Figure 3a). The plain washer faced the transmitter during the inspection. The second test piece is 14 mm thick and features two rectangular regions of different size where the foam core was removed entirely (see Figure 3b).

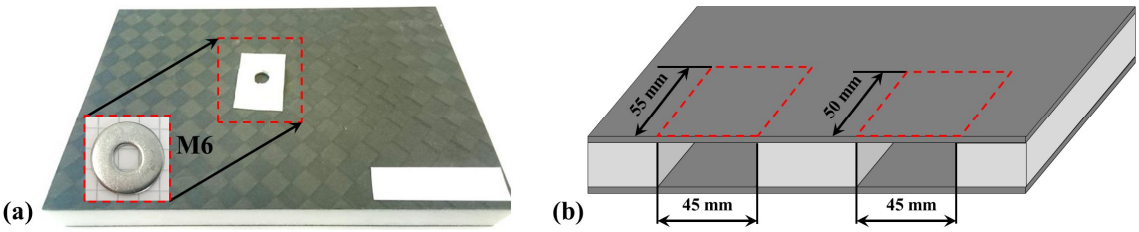

Figure 3. Two foam core sandwich test pieces with CFRP facesheets that are inspected in this study.

Figure 4 shows the recorded C-scan images of the first sandwich test piece. The C-scan recorded with the transducer pair displays the outer contour of the plain washer better (see Figure 4a). Note that, its inner bore can be resolved with the optical microphone and also the corners of the protruding rectangular tape can be estimated in Figure 4b.

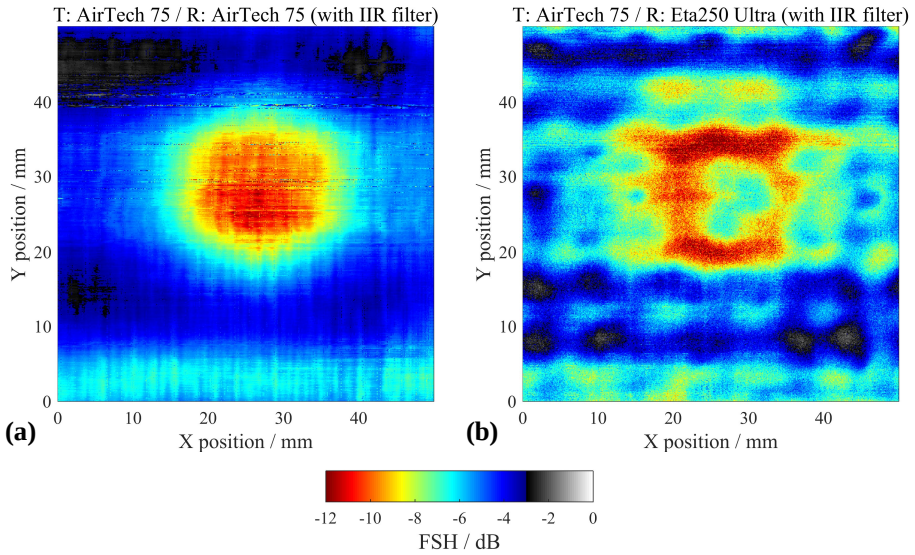

Figure 4. C-scan images of an M6 plain washer attached to the surface of a foam sandwich test piece using (a) a resonant receiver (AirTech 75) and (b) the optical microphone (Eta250 Ultra) for imaging.

Inspection results of the second sandwich composite are shown in Figure 5. The dynamic range of both C-scans differs significantly. Therefore, the starting point of each color scale was set to the average background noise in the respective C-scan and the transition point between black and blue to the -6 dB drop. Figure 5a shows a significantly higher signal-to-noise ratio (SNR) compared to Figure 5b. In the latter, however, the contrast of the edges to the surrounding material is higher and the corners appear much sharper.

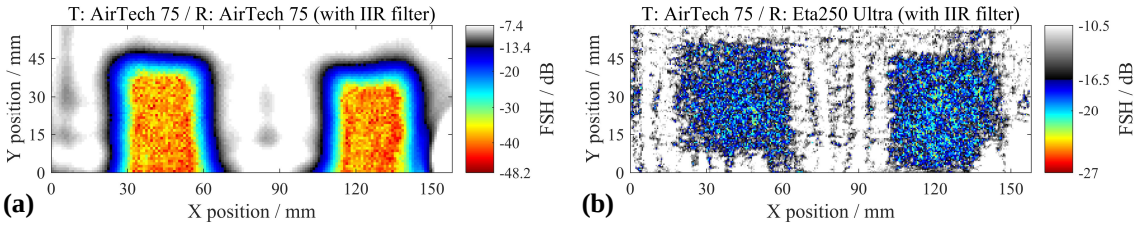

Figure 5. C-scan images of a sandwich test piece with missing foam core material using (a) a resonant receiver (AirTech 75) and (b) the optical microphone (Eta250 Ultra) for imaging.

Next, a 2 mm thick CFRP sample with induced impact damage is inspected. Therefore, three transmitter concepts are used to enable a very comprehensive evaluation of the optical receiver and its potential with novel actuator concepts. A uniform presentation of all recorded C-scan images is accomplished by defining the color scale the same way as before.

Figure 6 shows the C-scan images of the impact damage recorded with the resonant AirTech 200 transducer pair and the optical microphone. The probe characteristics and the applied filter parameters have already been described above.

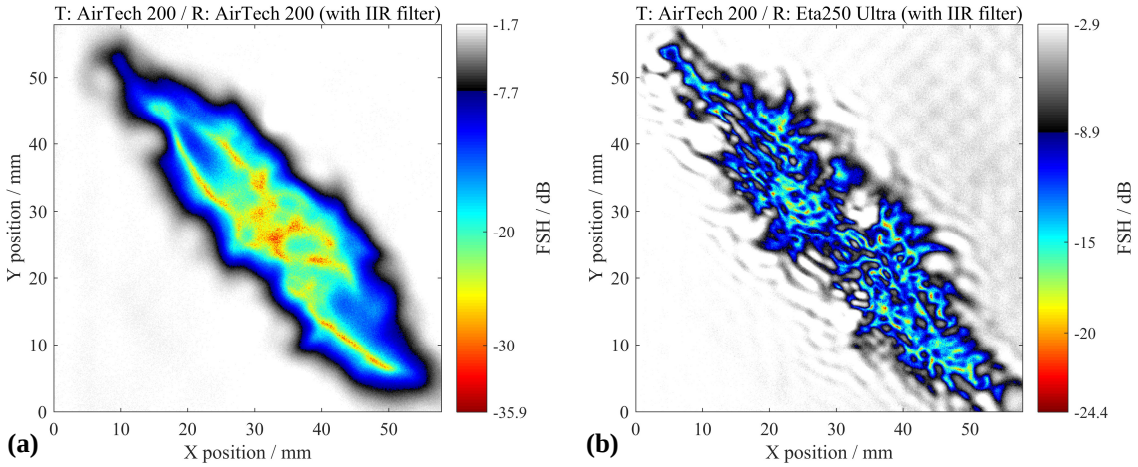

Figure 6. C-scan images of an impacted CFRP sample using (a) a resonant receiver (AirTech 200) and (b) the optical microphone (Eta250 Ultra) showing prominent interference and diffraction patterns.

The second setup consists of a ferroelectret transducer pair. The transmitter has a center frequency of 247 kHz and an aperture size of 19 mm. For a better spatial resolution, a receiver with an aperture size of 11 mm and a center frequency of 280 kHz was used. Both transducers have a normalized bandwidth of about 20 %. The results are shown in Figure 7a. In this test setup, the same transmitter could not be combined with the optical microphone as the transmitted sound pressure was too low for detection with the Eta250 Ultra. Therefore, the application of a ferroelectret transmitter with an aperture size of 27 mm, a lower center frequency (127 kHz) and bandwidth (about 16 %) was successful (see Figure 7b). The SNR was again improved by an eight-order IIR bandpass filter (105 kHz - 145 kHz).

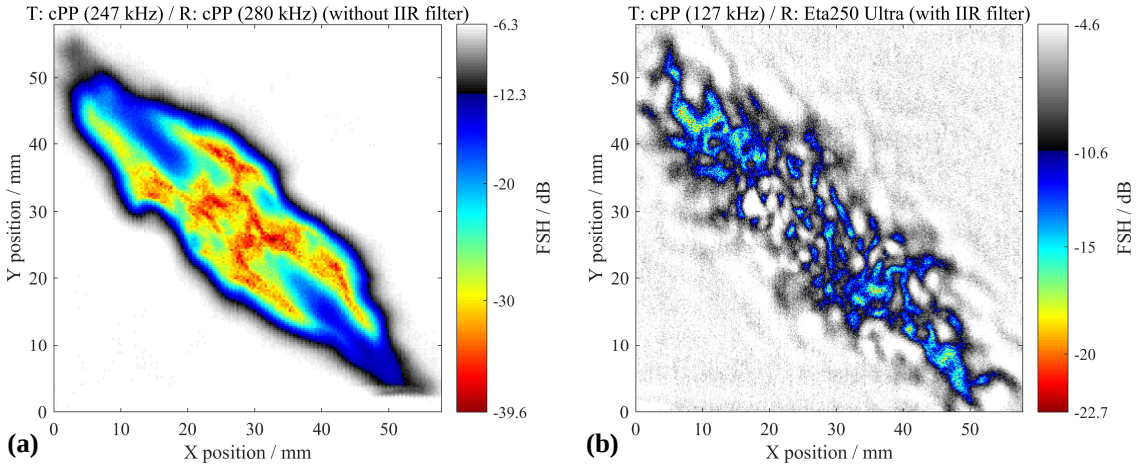

Figure 7. C-scan images of an impacted CFRP sample using (a) a pair of ferroelectret transducers with different center frequencies (T: 247 kHz and R: 280 kHz) and aperture sizes and (b) a ferroelectret transducer (T: 127 kHz) and the Eta250 Ultra showing prominent interference and diffraction patterns.

The optical microphones' tiny aperture can detect prominent interference and diffraction patterns in the C-scans shown in Figure 6b and 7b. They are caused by the complex structure of the present impact damage and mode conversion phenomena. Those patterns could not be resolved with the corresponding transducer pairs (see Figure 6a and 7a) and differ, depending on the probe characteristics, in terms of appearance and local occurrence. Impact loads to composite laminates can develop a complex damage structure consisting not only of fiber and matrix cracks but also of delaminations at

different depths. In combination with a quite narrowband ACU excitation, this can lead to local resonances in the through-transmission coefficient depending of the thickness of the impact-induced sublaminates. Hence, delaminated areas may not only cause signal drops of the through-transmission amplitude, whereby these patterns can occur (6, 16).

An investigation in our collaborative research group showed, that those characteristic structures could be reduced by adjusting the width of the measurement gate within the transmitted amplitude (17). The study of this phenomenon in greater detail, however, is the subject of further investigations.

Another possibility to diminish this dominant pattern in the C-scan images is the usage of new thermoacoustic transmitters. Due to their short broadband pulses, those actuators are not as prone to cause local thickness resonances as narrowband ACU probes. The impacted CFRP specimen was inspected using an ITO-based thermoacoustic transmitter (depicted in Figure 1b) and the optical microphone. An electrical square pulse lasting 4 µs at 400 V was used for ultrasound generation. The measured center frequency of this probe using these settings was 80 kHz with a bandwidth of over 100 %. To improve the SNR in the recorded C-scan image, signal averaging of the A-scan data of eight measurements was conducted. Due to the increased inspection duration, only the upper left section of the impacted CFRP specimen was inspected. The corresponding C-scan result is shown in Figure 8.

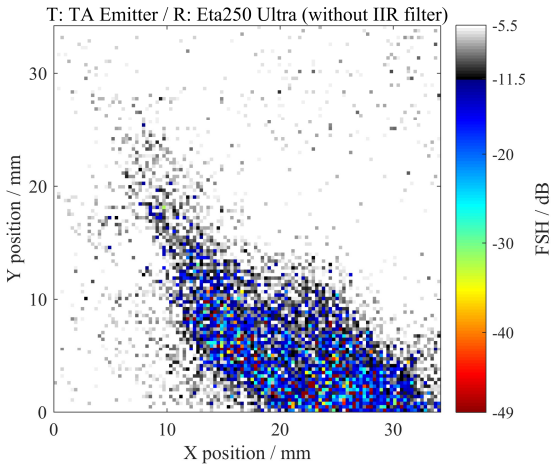

Figure 8. C-scan image of an impacted CFRP sample using an ITO-based thermoacoustic transmitter and the optical microphone (Eta250 Ultra).

Comparing Figure 8 with Figures 6 and 7 shows that the SNR is lower owing to the high bandwidth of the thermoacoustic transducer. Due to the narrow pulse width of the thermoacoustic transmitter, a broad acoustic spectrum, containing various higher frequencies, is stimulated. Two significant effects are limiting the imaging quality using a thermoacoustic emitter: first, the increased damping of higher frequencies by CFRP and; second, the limited bandwidth of a typical NDT system. The missing higher harmonics are causing a low receiving amplitude. Naturally, an increased signal amplitude is achieved by a higher amplification. Due to the gain increase, the noise is also amplified and the SNR is still kept low. Figure 8 indicates that the broadband excitation reduces the occurrence of the interference and diffraction patterns shown in Figures 6b and 7b. However, this cannot be conclusively verified due to the poor image quality. Ideally, a more sensitive version of the optical microphone must be used for verification.

5. Conclusions

The Eta250 Ultra demonstrated its applicability for modern ACU inspection, especially by improving the spatial resolution significantly. However, to fully exploit the optical microphones' potential combined with novel transmitter concepts, its sensitivity has to be optimized. This is possible during its manufacturing process (5). Combining this sensor with broadband thermoacoustic transmitters can also fulfill the need for a single-sided ACU pulse-echo standard configuration (9, 14).

Reasonable measurement results were usually obtained by necessarily choosing high analog and digital gain values at the ACU test instrument and the signal conditioning unit of the Eta250 Ultra. Therefore, the noise level in the microphone recorded C-scan images is generally high. An adjustment of the optical microphones' broad frequency range to the narrow spectrum of resonant transmitters with an IIR bandpass filter had a positive effect on the noise level of the recorded C-scans.

Narrowband transducers produced prominent interference and diffraction patterns in C-scans of an impacted CFRP sample. These wave phenomena could only be resolved by the small active aperture of the optical microphone. A test result using a broadband TA emitter indicates that these effects can be diminished, which can be beneficial, e.g. for defect sizing methods (6, 18).

Other results that were not presented in this contribution showed that this broadband optical sensor is also sensitive to surrounding sounds or reflections at objects within the laboratory. Unlike most other ultrasonic transducers, the open sensor is not only sensitive in the half-space in front of the aperture. Simple shieldings made of acoustic foam or frequency filters can be beneficial to the signal quality. In addition, the microphone was very effective to characterize sound fields of ACU transmitters.

Acknowledgements

The authors would like to thank Dr. Rainer Stößel from Airbus and Peter Jahnke from BMW who supported this study by providing some of the test pieces.

References

1. DE Chimenti: "Review of air-coupled ultrasonic materials characterization", Ultrasonics 54(7), pp 1804-1816, 2014.
2. W Hillger, R Oster, J Schuller, R Stößel, S Lang, J Bosse, B Thaler, D Ilse, L Bühling: "Automated Air-Coupled Ultrasonic Technique for the Inspection of the EC145 Tail Boom", 4th International Symposium on NDT in Aerospace, Augsburg/Germany, 2012.
3. W Hillger, L Bühling, D Ilse: "Air-coupled Ultrasonic Testing-Method, System and practical Applications", 11th European Conference on Non-Destructive Testing (ECNDT), Prague, 2014.
4. VM Karbhari: "Non-Destructive Evaluation (NDE) of Polymper Matrix Composites – Techniques and Applications", Woodhead Publishing Limited, Cambridge, ISBN: 978-0-85709-344-8, 2013.
5. E Guruschkin: "Berührungslose Prüfung von Faserverbundwerkstoffen mit Luftultraschall", Master's thesis, Technical University of Munich (Chair of Non-destructive Testing), 2015.
6. CU Grosse, M Goldammer, J-C Grager, G Heichler, P Jahnke, P Jatzlau, D Kiefel, R Oster, MGR Sause, R Stößel, M Ulrich: "Comparison of NDT Techniques to Evaluate CFRP – Results Obtained in a MAIzfp Round Robin Test", 19th World Conference on Non-Destructive Testing (WCNDT), Munich/Germany, 2016.
7. M Gaal, J Döring, J Bartusch, T Lange, W Hillger, G Brekow, M Kreutzbruck: "Ferroelectret Transducers For Air-Coupled Ultrasonic Testing of Fiber-Reinforced Polymers", AIP Conf. Proc. 1511, The 39th Annual Review of Progress in Quantitative Nondestructive Evaluation (2012), pp 1534-1540, Denver/Colorado (USA), 2013.

8. M Gaal, J Bartusch, E Dohse, F Schadow, E Köppe: “Focusing of Ferroelectret Air-Coupled Ultrasound Transducers”, AIP Conf. Proc. 1706, The 42nd Annual Review of Progress in Quantitative Nondestructive Evaluation (2015), Minneapolis/Minnesota (USA), 2016
9. M Gaal, J Bartusch, F Schadow, U Beck, M Daschewski, M Kreutzbruck: „Airborne ultrasonic systems for one-sided inspection using thermoacoustic transmitters”, 2016 IEEE International Ultrasonics Symposium (IUS), Tours/France, 2016.
10. K Nakamura: “Ultrasonic Transducers – Materials and Design for Sensors, Actuators and Medical Applications”, Woodhead Publishing Limited, Cambridge, ISBN: 978-1-84569-989-5, 2012.
11. R Stößel: “Air-Coupled Ultrasound Inspection as a New Non-Destructive Testing Tool for Quality Assurance”, PhD Thesis, University of Stuttgart (Institut für Kunststofftechnik), 2004.
12. R Steinhausen, M Kiel, C Pientschke, H-J Münch, A Mück, K Hahn: “New approaches to air-coupled ultrasound testing of composite lightweight materials”, 19th World Conference on Non-Destructive Testing (WCNDT), Munich/Germany, 2016.
13. TE Gómez Álvarez-Arenas, J Camacho, C Fritsch: “Passive focusing techniques for piezoelectric air-coupled ultrasonic transducers”, Ultrasonics 67, pp 85-93, 2016.
14. M Gaal, M Daschewski, J Bartusch, F Schadow, E Dohse, M Kreutzbruck, M Weise, U Beck: “Novel air-coupled ultrasonic transducer combining the thermoacoustic with the piezoelectric effect”, 19th World Conference on Non-Destructive Testing (WCNDT), Munich/Germany, 2016.
15. B Fischer: “Optical Microphone hears ultrasound”, Nature Photonics 10, pp 356-358, 2016.
16. W Hillger, R Meier, R Henrich: “Inspection of CFRP components by ultrasonic imaging with aircoupling”, Insight – Non-Destructive Testing and Conditioning Monitoring 46(3), pp 147-150, 2004.
17. J Gamper: “Entwicklung eines neuen Messkonzepts zur luftgekoppelten Ultraschallprüfung von Faserverbundwerkstoffen“, Master’s thesis, Technical University of Munich (Chair of Non-destructive Testing), 2017.
18. F Schadow, D Brackrock, M Gaal, T Heckel: “Ultrasonic Inspection and Data Analysis of Glass- and Carbon-Fibre-Reinforced Plastics“, Procedia Structural Integrity (7), pp 299-306, 2017.